ELSEVIER

Ceramics International 30 (2004) 229–238

CERAMICS INTERNATIONAL

www.elsevier.com/locate/ceramint

Microstructural development of Y-α/(β)-sialons after post heat-treatment and its effect on mechanical properties

Feng Ye[a,*], Michael J. Hoffmann[b], Stefan Holzer[b], Mikio Iwasa[c]

[a]*School of Materials and Engineering, Harbin Institute of Technology, Harbin 150001, PR China*
[b]*Institute of ceramics in Mechanical Engineering, University of Karlsruhe, D-76131 Karlsruhe, Germany*
[c]*National Institute of Advanced Industrial Science and Technology, AIST Kansai, Ikeda, Osaka 563-8577, Japan*

Received 2 January 2003; received in revised form 8 April 2003; accepted 20 April 2003

Abstract

Dense Y-α and duplex Y-α/β-sialon ceramics were fabricated by hot isostatic pressing (HIP) using the compositions with the formula $Y_{m/3}Si_{12-(m+n)}Al_{m+n}O_nN_{16-n}$ and extra addition of 2 wt.%Y_2O_3. The sintered materials were subsequently heat-treated at 1300–1700 °C to investigate the thermal stability of Y-sialons. The results show that α-sialon stabilized by yttrium has high thermal stability. An adjustment of α-sialon phase composition is the dominating reaction during annealing. Post heat-treatment has a little effect on the microstructure and properties of the Y-α/β-sialons, but significantly changes the morphology of α-phase grains in Y-α-sialons from elongated to equiaxed after heat-treatment at 1500 °C for extended time, hence decreasing its toughness.

Keywords: B. Microstructure; C. Mechanical properties; D. Sialon; Post heat-treatment

1. Introduction

Sialon ceramics offer the advantage of easier fabrication compared with S_3N_4 ceramics because of the lower viscosity of M–Si–Al–O–N liquid phase, which facilitates easier densification at sintering temperatures. Another advantage is that the amount of intergranular phase can be reduced if the transient liquid phase is absorbed into the matrix forming α-sialon phase in the final product.

The two most important sialon phases, α and β, have structures based on α- and β-Si_3N_4 with aluminum and oxygen partially replacing silicon and nitrogen. α-sialon has the general formula $M_xSi_{12-(m+n)}Al_{(m+n)}O_nN_{16-n}$, where M is a metal ion typically Li, Mg, Ca, Y and Ln, β-sialon on the other hand, does not incorporate other cations. The composition of this phase is given by the formula $Si_{6-z}Al_zO_zN_{8-z}$, with Z varying from 0 (Si_3N_4) to a maximum value of about 4.2 depending on sintering condition [1–3].

Duplex α/β-sialon ceramics offer possibilities of tailoring the microstructure, for example, equiaxed α-sialon grains can be matched with elongated β-sialon grains to form a toughened composites, and consequently the properties of the final product can be improved, because they combine the high fracture toughness of β-sialon with the good hardness of α-sialon. Another advantage is that densification of duplex α/β-sialon is much easier than pure α-sialon. Therefore, by varying the overall composition in the M–Si–Al–O–N system, it is possible to vary the α:β sialon phase ratio of sintered ceramics in a controlled way, and hence will give rise to a series of materials where hardness and fracture toughness can be tailored [4–6].

Thompson et al. [7–9] have reported that the phase content of a certain α/β-sialon composition can be greatly affected by heat-treatment procedures where rare earth oxides are used as the sintering aid. The α-sialon phase is less stable at low temperature and decomposes into rare-earth-rich intergranular phase and the β-sialon. The thermal stability of the α-sialon phase depends on the starting composition, type of additives, the amount and viscosity of liquid phase, and the presence or absence of β-sialon grains in the initial sintered material. Therefore, a complete understanding the mechanism of this interesting transformation during heat-treatment is essential to define more precisely safe operating conditions for sialon ceramics. On the other

* Corresponding author at current address: National Institute of Advanced Industrial Science, Technology, AIST Kansai, Midorigaoka 1-8-31, Ikeda, Osaka 563-8577, Japan.

0272-8842/03/$30.00
doi:10.1016/S0272-8842(03)00094-4

hand, this transformation could undoubtedly provide an excellent mechanism for optimizing phase content and microstructure without further additions of oxides and nitrides, merely by heat-treatment at appropriately chosen temperatures.

In this study, α- or duplex α/β-sialon starting compositions are densified by hot isostatic pressing (HIP) using yttria. The resulting materials were heat-treated at 1300 to 1700 °C to clarify the thermal stability of Y-sialons. The effects of composition and post heat-treatment on α→β-sialon transformation, microstructure and mechanical properties were investigated.

Table 1
Starting compositions of Y-sialon ceramics (wt%)

Sample	Si_3N_4	Al_2O_3	AlN	Y_2O3	TD (g/cm^3)	RD (%)
Y1010-E2	77.873	0.228	13.517	8.381	3.293	98.809
Y0810-E2	80.229	0.817	11.793	7.160	3.280	98.753
Y0610-E2	82.635	1.421	10.034	5.909	3.268	99.564
Y0410-E2	85.097	2.041	8.235	4.625	3.254	99.583
Y0210-E2	87.600	2.670	6.403	3.330	3.241	99.762

2. Experimental procedure

The overall starting compositions are listed in Table 1. The chemical compositions are defined by the formula $Y_{m/3}Si_{12-(m+n)}Al_{m+n}O_nN_{16-n}$. For the selected compositions, an extra 2 wt.% Y_2O_3 was added to achieve complete densification. Throughout the work, we will refer to these compositions as Y-10m10nE2. For instance, Y0210E2 represents the materials with $m=0.2$, $n=1$ and 2 wt.% excess additions of Y_2O_3. Starting powders were Si_3N_4 (E10 Grade, UBE Industries Ltd,Japan), AlN (Grade C, H. C. Starck, Germany), Al_2O_3 (Grade A16SG, Alcoa) and Y_2O_3 (Grade fine, H.

Table 2
Phase compositions and lattice parameters of Y-sialons before and after heat treatment

Material	Phase composition (wt.%)			α-sialon			β-sialon		
	α	β	Other phases	a_α (nm)	c_α (nm)	x	a_β (nm)	c_β (nm)	z
HIP,1800 °C,1 h									
Y0210E2	38	62		0.7797	0.5678	0.33	0.7622	0.2923	0.63
Y0410E2	68	32		0.7799	0.5677	0.33	0.7625	0.2924	0.70
Y0610E2	82	18		0.7799	0.5681	0.35	0.7625	0.2924	0.70
Y0810E2	100	vw*		0.7803	0.5681	0.36			
Y1010E2	100	0		0.7803	0.5683	0.36			
HT, 1700 °C, 10 h									
Y0210E2	37	63		0.7796	0.5678	0.33	0.7618	0.2921	0.53
Y0410E2	68	32		0.7795	0.5676	0.32	0.7618	0.2921	0.53
Y0610E2	81	19		0.7797	0.5677	0.33	0.7619	0.2920	0.52
Y0810E2	100	vw		0.7800	0.5680	0.35			
Y1010E2	100	0		0.7803	0.5684	0.36			
HT, 1300 °C, 10 h									
Y0210E2	35	65		0.7792	0.5675	0.31	0.7619	0.2920	0.52
Y0410E2	68	32		0.7796	0.5673	0.31	0.7622	0.2916	0.57
Y0610E2	82	18		0.7797	0.5680	0.33	0.7623	0.2921	0.61
Y0810E2	100	vw		0.7801	0.5679	0.35			
Y1010E2	100	0		0.7800	0.5681	0.35			
HT, 1500 °C, 10 h									
Y0210E2	36	64		0.7791	0.5674	0.30	0.7618	0.2920	0.51
Y0410E2	63	37		0.7794	0.5672	0.30	0.7619	0.2921	0.54
Y0610E2	80	20	M'(vw)	0.7792	0.5678	0.31	0.7619	0.2919	0.50
Y0810E2	100	vw	M'(vw)	0.7800	0.5679	0.34			
Y1010E2	100	0	M'(vw)	0.7798	0.5680	0.34			
HT, 1500 °C, 74 h									
Y0210E2	31	69		0.7791	0.5676	0.30	0.7616	0.2918	0.43
Y0410E2	59	41		0.7793	0.5673	0.30	0.7617	0.2918	0.45
Y0610E2	72	28	M'	0.7792	0.5673	0.30	0.7616	0.2919	0.45
Y0810E2	96	4	M'	0.7798	0.5677	0.33			
Y1010E2	100	0	M'	0.7799	0.5680	0.34			

C. Starck, Germany). When calculating the overall compositions, 2.42 wt.% SiO_2 and 3.4 wt.% Al_2O_3 (according to manufacturer's specifications) on the surface of Si_3N_4 and AlN powders respectively were taken into account.

The starting materials were wet milled in a planetary mill in isopropanol for 8 h with silicon nitride balls as the mixing media. The powder mixtures were subsequently dried at 40 °C in a rotary evaporator and sieved. Consolidation of the powders to rectangular plates (65×45×5 mm) was obtained by uniaxial pressing in a steel die at a pressure of 17 MPa and subsequent cold isostatic pressing at 600 MPa. The green pellets were hot isostatic pressed at 1800 °C for 1 h under a pressure of 1 MPa.The temperature was raised at a rate of 30 °C/min. After the completion of densification, the furnace was switched off to allow rapid cooling. The cooling rate was about 100 °C/min. The densities of the sintered specimens were measured by Archimedes' method.

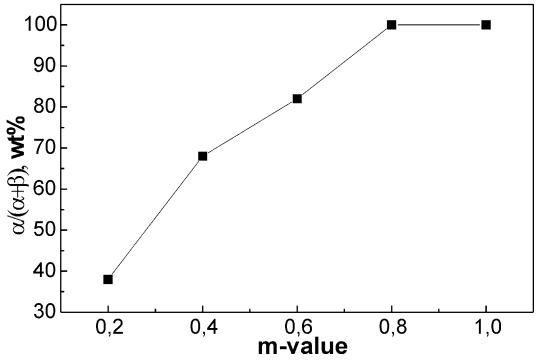

Fig. 1. α/(α + β)-sialon ratios of HIP-sintered Y-sialons as a function of *m*-value.

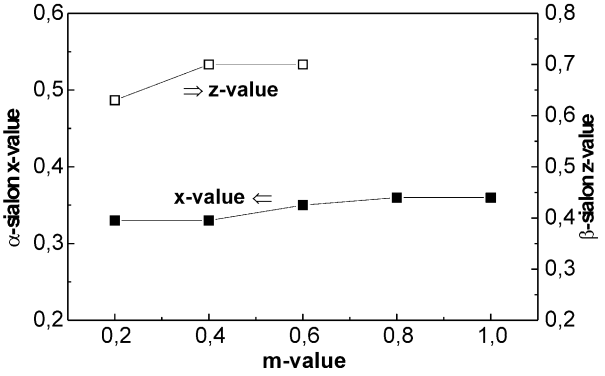

Fig. 2. α-sialon *x* value and β-sialon *z* value of HIP-sintered Y-sialons.

The sintered specimens were post heat-treated at 1300–1700 °C for 10–74 h in nitrogen atmosphere to examine the thermal stability of the investigated Y-sialons.

Before and after heat treatment the crystalline phases of investigated sialons were characterized by X-ray diffraction (XRD). The amounts of α- and β-sialon phases were determined using the intensities of the (102) and (210) reflections of α-sialon and (101) and (210) reflections of β-sialon [9]. The *x* values of α-sialon phases $M_xSi_{12-(m+n)}Al_{(m+n)}O_nN_{16-n}$were obtained from the mean values of x_a and x_c in the follow relations [10]:

$$a\ (\text{nm}) = 0.775 + 0.0156\ x_a \quad (1)$$

$$c\ (\text{nm}) = 0.562 + 0.0162\ x_c \quad (2)$$

The *z* values of β-sialon phases $Si_{6-z}Al_zO_zN_{8-z}$ were determined from the mean values of z_a and z_c given by the following equations [3]:

$$a\ (\text{Å}) = 7.603 + 0.0297 z_a \quad (3)$$

$$c(\text{Å}) = 2.907 + 0.0255 z_c \quad (4)$$

After application of a carbon coating, the polished surfaces of sintered and heat-treated samples were examined by scanning electron microscope (SEM) using backscattered electron mode (BSE) for imaging.

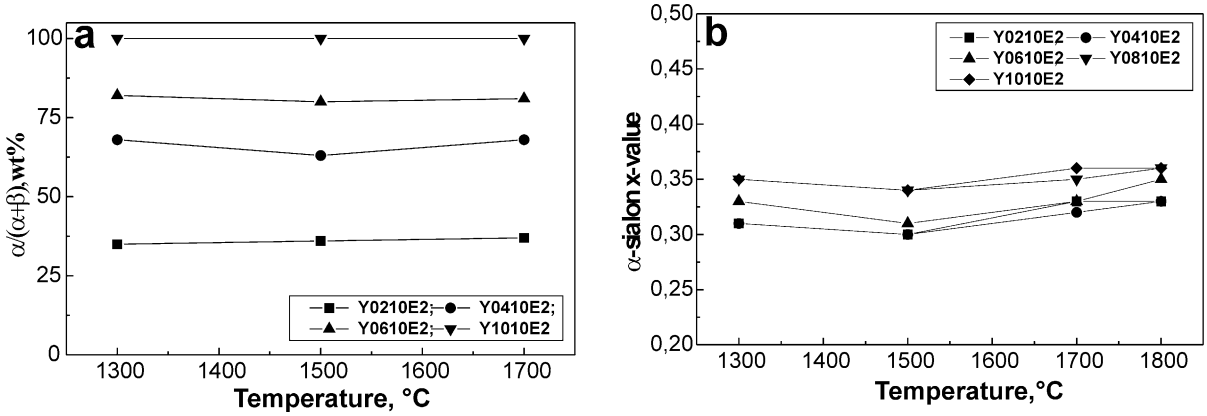

Fig. 3. The α-sialon phase contents and *x* value of Y-sialons after heat treatment at different temperatures for 10 h. (a) α-sialon phase content; (b) α-sialon *x* value.

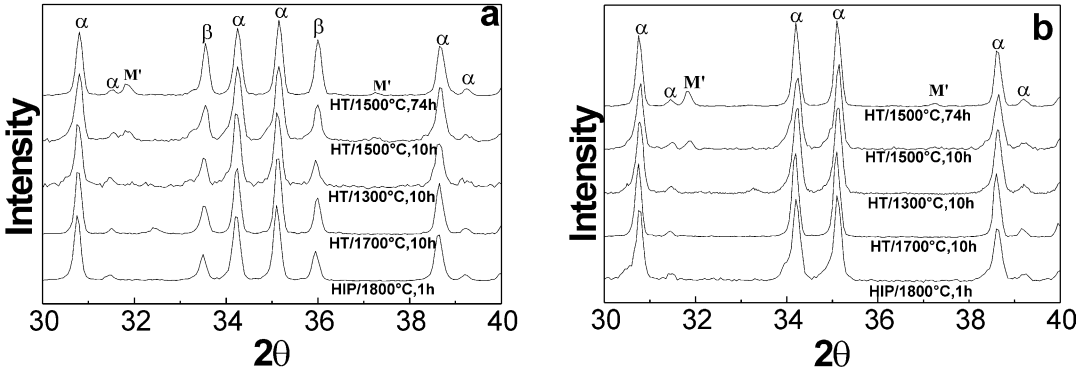

Fig. 4. XRD patterns of the Y-sialons before and after heat treatment. (a)Y0610E2, (b) Y1010E2.

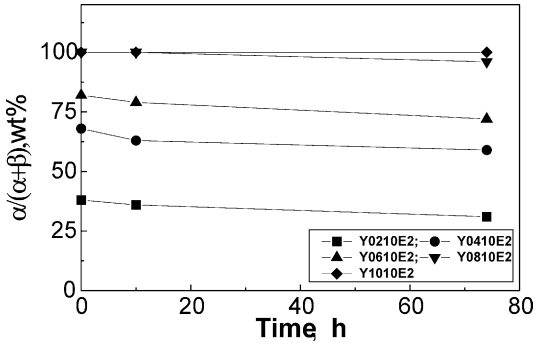

Fig. 5. The α-sialon phase contents of Y-sialons after heat-treatment at 1500 °C for 10 up to 74 h.

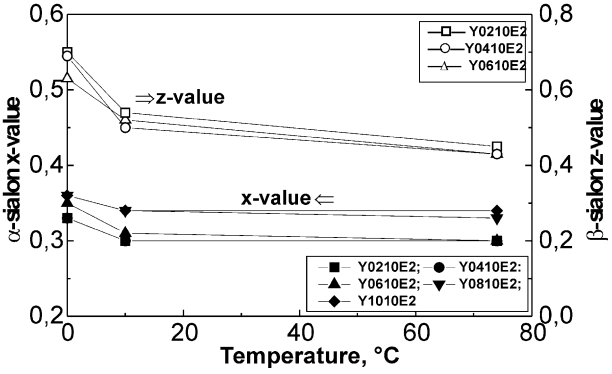

Fig. 6. α-sialon x value and β-sialon z value after heat treatment at 1500 °C for 10 up to 74 h.

Hardness (H_{V10}) and indentation fracture toughness (K_{IC}) were determined by a Vickers diamond indenter with a 98 N load. K_{IC} was calculated by the method of Anstis et al. [11], assuming a Young's modulus of 300 GPa.

3. Results and discussion

3.1. Phase analysis

All sintered samples were densified to ~99% of the theoretical value, as shown in Table 1, indicating that excess Y_2O_3 effectively promotes Y-sialons densification.

Phase composition and unit cell dimension of the Y-sialons after sintering and heat-treatment are shown in Table 2. Only α- and/or β-sialon phases were observed in all the sintered samples. No secondary crystalline phases were detected by XRD, indicating that the cooling rate is sufficient to prevent crystallization of any grain boundary glass during cooling. The α-sialon content increases with m value, which is expected from the phase diagram, as shown in Fig. 1. The unit cell dimensions of both the α-and β-phase also slightly increase with m value (Fig. 2).

The effects of post heat-treatment on the phase content of the Y-stabilized sialons are shown in Fig. 3. It reveals that the content of α-sialon phase and its x value depends on the annealing temperature. The most critical temperature seems to be around 1500 °C. Heat-treating the duplex Y-α/β-sialons at 1500 °C for 10h resulted in a slow decrease in α-phase content and a simultaneously increase of the β-phase content. An initial formation of a small amount of Y–M' phase was accompanied by small reductions in α-sialon x-value (as shown in Figs. 3 and 4), possibly as the result of a reaction between the liquid and α- and β-sialon phase in order to compensate for the composition difference between the Y–M' phase and the glass phase present prior to the heat treatment. For Y-α-sialon material (i.e. Y1010E2), there was no α→β-sialon phase transformation, although M' phase also was detected after heat-treating at 1500 °C for 10 h.

The phase contents of Y-sialons after heat treatment at 1500 °C for different times are shown in Fig. 5. Extending heat-treatment time to 74 h, the Y-α/β-sialons show a further small shift of α to β phase, but the overall composition of α-sialon phase is constant and the z value of β-sialon phase shows a decrease (as shown in Fig. 6). However, for Y-α-sialon sample (i.e. Y1010E2), still no α to β phase transformation was detected during the prolonged heat-treatment. Although

the M' phase content slightly increases with time, it has no obvious effect on phase composition and substitution level. So it can be concluded that the formation of the Y–M' phase is mainly contributed to the devitrification of the grain boundary liquid phase. When Y-α-sialons were prepared from stoichiometric compositions, no M' phase formation was observed, even after annealing at 1450 °C for 30 days [4]. Therefore, in present study, the M' phase formation in Y-α-sialon during heat treatment may be due to the incorporation of extra Y_2O_3 into the starting compositions, which provides Y needed for Y–M' phase formation.

As stated above, the α-sialon phase stabilized by yttrium has high thermal stability. The adjustment of

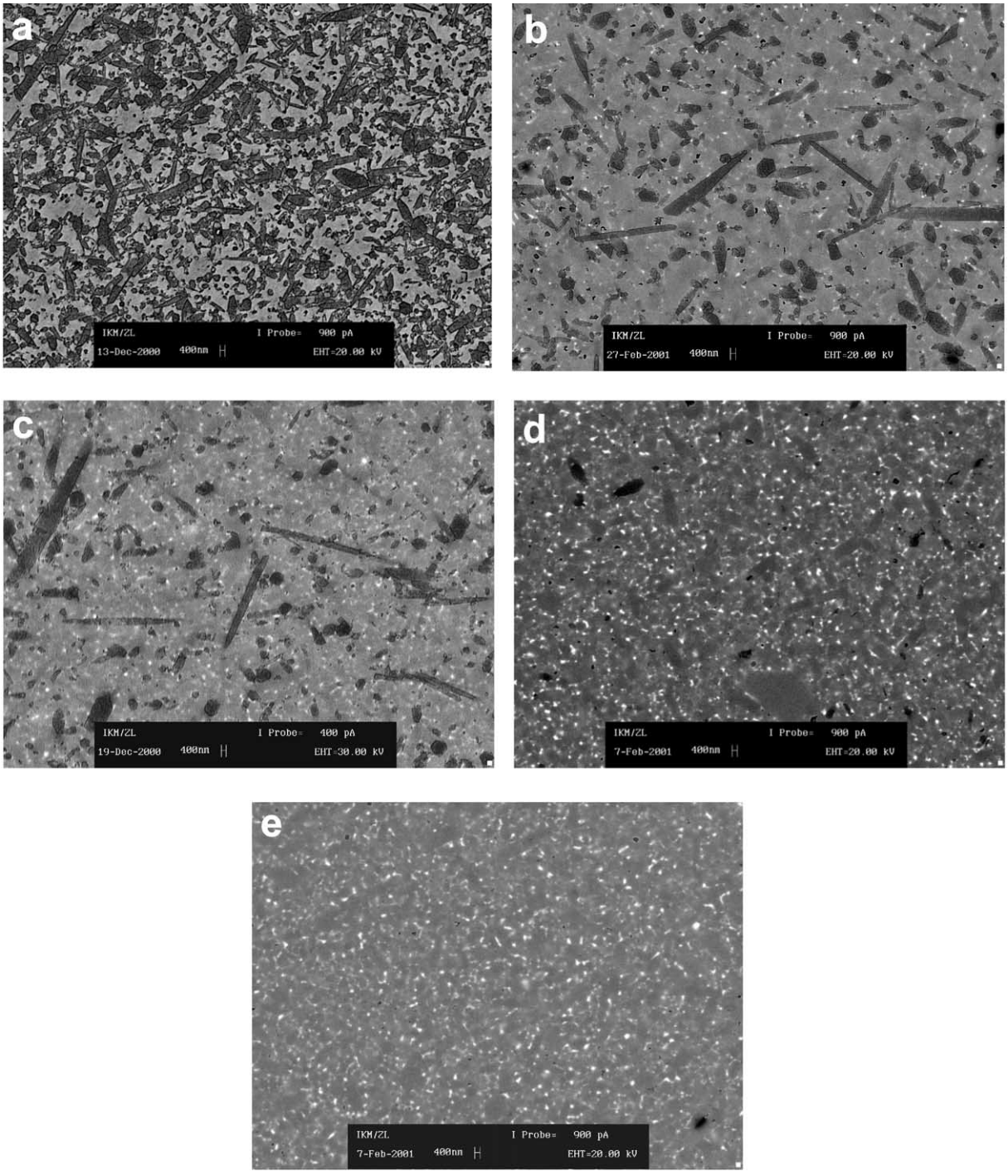

Fig. 7. SEM micrographs (back-scatted mode) of Y-sialons HIP-sintered at 1800 °C for 1 h: (a) Y0210E2, (b) Y0410E2, (c) Y0610E2, (d) Y0810E2, (e) Y1010E2.

α-sialon phase composition is the dominant reaction in the Y-α/(β)-sialons during post heat-treatment, possibly according to the following reaction:

$$\alpha_1 + \text{grain boundary liquid} \rightarrow \alpha_2 + \text{M'} \quad (5)$$

where α_2 is an α-sialon phase with a lower×value than that of α_1 because the formation of Y–M' phase will consume yttrium from both the liquid and the α-sialon.

3.2. Effect of heat treatment on the microstructure of Y-sialons

The microstructures of the Y-sialons after HIP-sintering are shown in Fig. 7, where the β-sialon grains are black and needlelike, whereas the α-sialon grains are grey and equiaxed, and the grain boundary phases are bright because they contain more Y than α or β phases. The

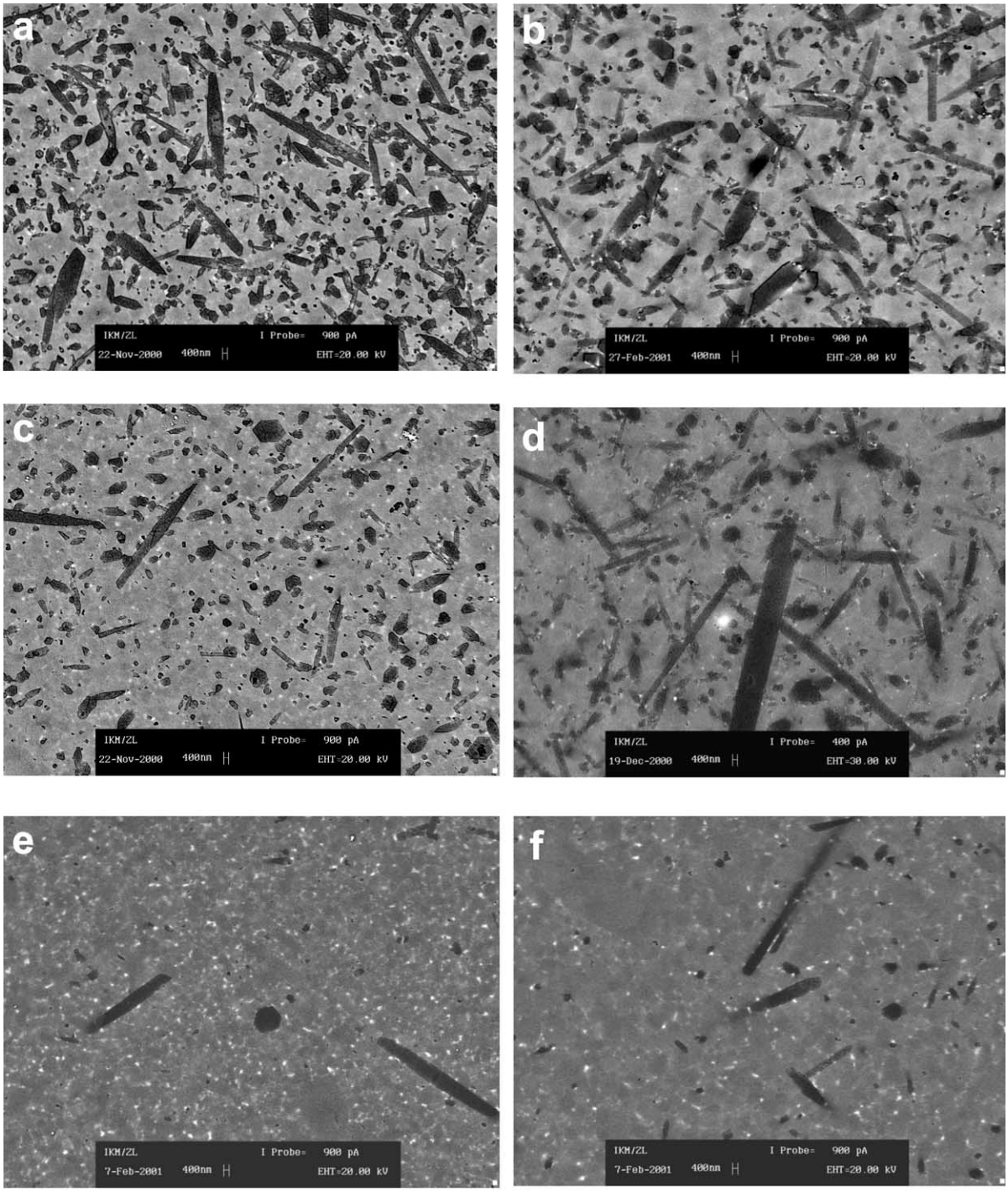

Fig. 8. SEM micrographs (back-scatted mode) of Y-α/β-sialons after heat treatment. (a) Y0410E2,1500 °C, 10 h; (b) Y0410E2, 1500 °C, 74 h; (c),Y0610E2, 1500 °C,10 h; (d) Y0610E2, 1500 °C,74 h; (e) Y0810E2, 1500 °C,10 h; (f) Y0810E2, 1500 °C, 74 h.

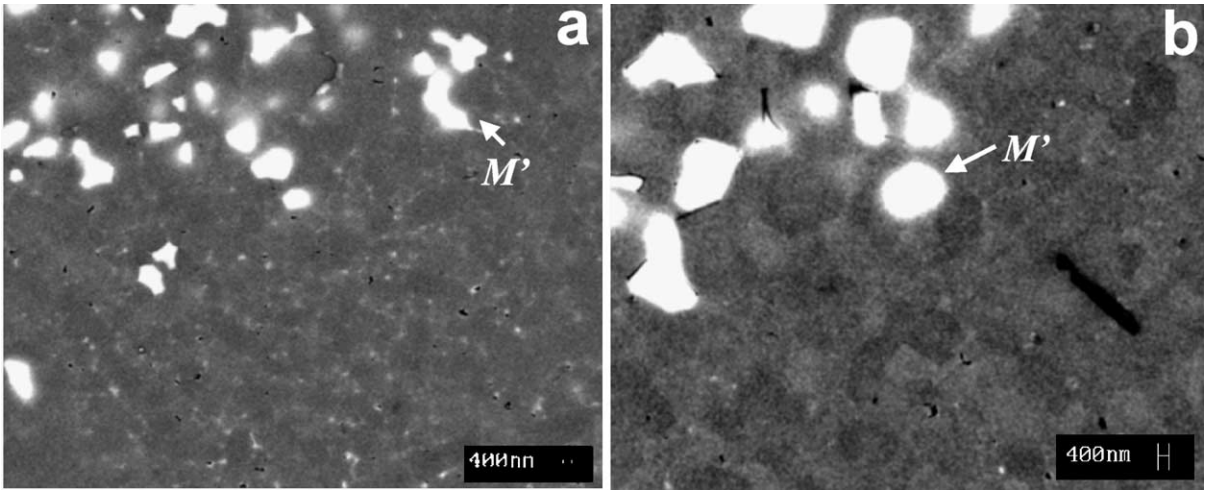

Fig. 9. SEM micrographs (BSE mode) of Y-α-sialon sample after heat treatment. (a) 1500 °C, 10 h; (b) 1500 °C, 74 h.

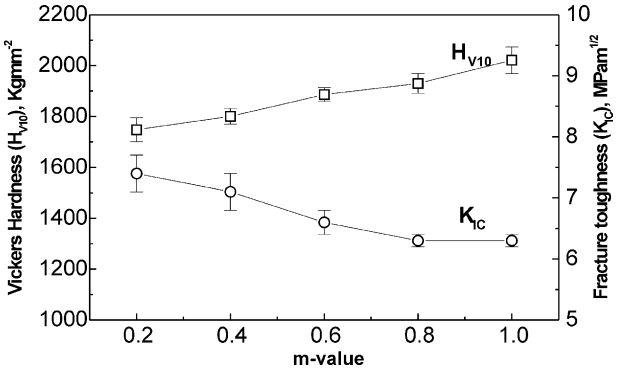

Fig. 10. Indentation fracture toughness (K_{IC}) and Vickers hardness (H_{V10}) of Y-sialons HIP-sintered at 1800 °C for 1 h versus *m*-value.

volume fraction of intergranular phase decreases with increasing β-sialon content. The decrease may be explained by the presence of two sialon phases with extended solid solutions and resulting in the ability to locally accommodate smaller variations in chemistry.

For duplex Y-α/β-sialons (Fig. 7a, b and c), the aspect ratio of β phase grain increases with increasing α-sialon content. Indeed a high α-sialon content can provide a large amount of transient liquid during sintering, which should facilitate the growth of β-sialon grain.

The most interesting result of SEM observations is the presence of α-sialon with many elongated grains in Y0810E2 and Y1010E2 samples, as shown in Fig. 7d and e. Elongated α-sialon grains have been observed in other α-sialon ceramics [12–16]. The results indicated that the formation of elongated α-sialon grains could be favored by the presence of liquid phase supersaturated in α-sialon constituents at the sintering temperature. The effect of amount of additives on the microstructure of Y-α-sialon ceramics will be described in another paper. The effect of elongated α-sialon grains on the mechanical properties will be discussed in next section.

The microstructures of Y-α/β-sialon materials after heat treatment at 1500 °C are shown in Fig. 8 which reveals that the microstructure of duplex sialons underwent coarsening and the β-sialon phase content slightly increased after heat treatment at 1500 °C for 10 h (Fig. 8a, c and e). Further extending the heat-treatment time to 74 h, their microstructures were stable and did not change obviously, as shown in Fig. 8b, d and f.

For Y-α-sialon sample (Y1010E2), after annealing at 1500 °C for up to 74 h, there is still no α→β-sialon transformation, Table 2, which is consistent with the XRD results, but its microstructure changes very much in the morphologies of grain boundary phase and α phase grain, as shown in Fig. 9. After heat treatment at 1500 °C for 74 h, the α-sialon grains are not elongated, but equiaxed. The boundaries between adjacent α-sialon grains are almost invisible, giving the matrix a very uniform appearance (Fig. 9b) which further confirms that the formation of M' phase is attributed to the crystallization of the glassy phase.

3.3. Mechanical properties

The Vickers hardness (H_{V10}) and indentation fracture toughness (K_{IC}) of the investigated Y-sialons are summarized in Fig. 10. As indicated, with increasing the *m*-value, i.e. increasing α-sialon phase contents in the final materials, the fracture toughness decreases and the hardness increases, due to the high fracture toughness of β-sialon phase and the good hardness of α-sialon. The main toughening mechanisms in the duplex Y-α/β-sialons are crack deflection and elongated β-grain pullout, which can be demonstrated clearly by the indentation crack propagation path, as shown in the Fig. 11a.

Fig. 10 also reveals that the investigated Y-α-sialons also possess high toughness, the toughness of both Y1010E2 (pure α-sialon) and Y0810E2 (with little β phase) sample are over 6.0MPam$^{1/2}$. This is attributed

to the formation of elongated α-sialon grains (Fig. 7d and e) whose crack propagation paths are shown in Fig. 11c and e, respectively. It clearly reveals the crack deflection and elongated α-sialon grain pullout during fracturing.

The mechanical properties of Y-sialon ceramics after heat treatment at 1500 °C are summarized in Fig. 12. The hardness decreased slightly with heat-treatment time (Fig. 12a) and is dependent on the volume fractions and hardness of the constituent phases. Undoubtedly, the increase in the amount of β-sialon and the formation of M' phase during heat-treatment lead to the observed decrease in hardness of Y-sialons because the hardness of α-sialon (around 22 GPa) is higher than that of the formed two phases (H_{V10}≈17 GPa for β-sialon and H_{V10}≈9 MPa for M' phase).

There are no obvious changes in the indentation fracture toughness of the duplex α/β-sialons (Y0210E2, Y0410E2 and Y0610E2 samples) after heat-treatment at 1500 °C, as shown in Fig. 12b, possibly because the heat-treatment did not cause any significant change in their microstructure (Figs. 7 and 8). The indentation crack propagation path also showed that the propagating crack deflected along the α/β interface, Fig. 11b. However, for pure α-sialon sample (Y1010E2), the fracture toughness decreased from 6.3 to 5.3 MPam$^{1/2}$

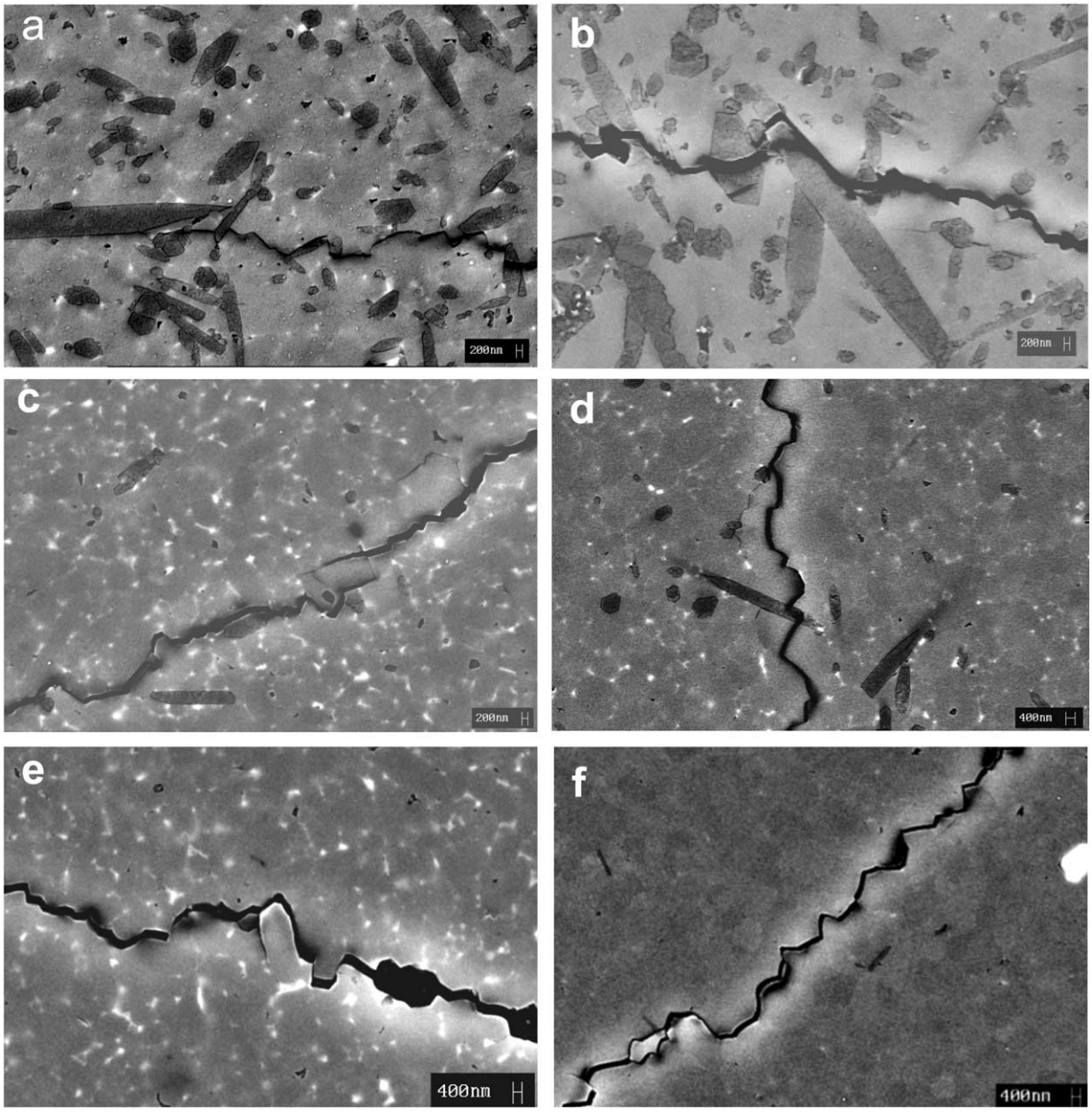

Fig. 11. Indentation crack propagation paths of Y-sialons before and after heat treatment. (a) Y0410E2, HIP; (b) Y0410E2, 1500 °C, 74 h; (c)Y0810E2, HIP; (d) Y0810E2, 1500 °C, 74 h; (e) Y1010E2, HIP; (f) Y1010E2, 1500 °C, 74 h.

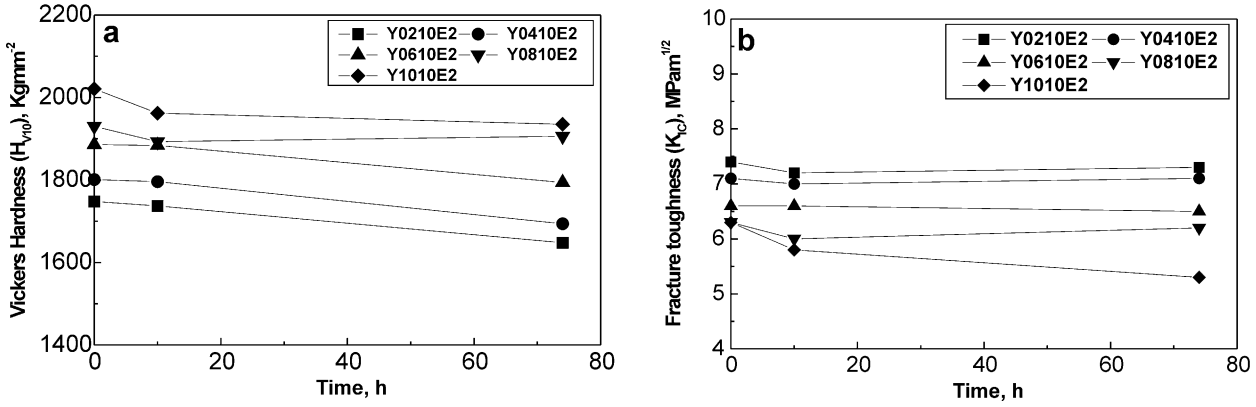

Fig. 12. Mechanical propreties of Y-sialons heat-treated at 1500 °C, as functions of heat-treatment time. (a) Vickers hardness; (b) fracture toughness.

after heat-treatment at 1500 °C for 74 h. It is attributed to the altered α-sialon morphology. The initial whisker-like microstructure would promote crack deflection during fracturing and hence high fracture toughness. For Y0810E2 sample, although the morphology of α-sialon grains are also strong influenced by the post heat-treatment, the increase in the amount of β-sialon with elongated grain after prolonged heat treatment could compensate the decrease in toughness caused by the shape change of α-sialon grain, as shown in Fig. 11d.

4. Conclusions

1. Dense Y-α/(β)-sialon ceramics can be prepared by HIPing with incorporation of excess yttria.
2. Y-α-sialon phase is stable during heat treatment in the temperature range 1300–1700 °C. An adjustment of α-sialon phase composition is the dominant reaction during the heat- treatment.
3. Elongated α-sialon grains were found in the pure Y-α-sialon materials after HIP-sintering which may be attributed to the addition of excess yttria into the starting composition. The elongated grains promote the crack deflection and grain pullout effects.
4. Prolonged heat treatment at 1500 °C has little influence on the mechanical properties of duplex Y-α/β-sialons because the microstructure is unaffected by the heat treatment. However, the initially elongated α-sialon grains in the pure α-sialon tend to become equiaxed after the heat treatments, hence decreasing its toughness.

Acknowledgements

Dr. Feng Ye acknowledges financial assistance from Alexander von Humboldt Foundation (AvH, Germany) during the period when the work was carried out. He also thanks Mrs. R. Satet and Mr. Müller at Karlsruhe University who have contributed to some aspects of this work.

References

[1] L.J. Gauckler, H.L. Lukas, G. Petzow, Contribution to the phase diagram Si_3N_4–AlN–Al_2O_3–SiO_2, J. Am. Ceram. Soc. 58 (1975) 346–348.
[2] K.H. Jack, The signification of structure and phase equilibria in the development of silicon nitride and sialon ceramics, Sci. Ceram. 11 (1981) 125–142.
[3] T. Ekström, P.O. Käll, M. Nygren, P.-O. Olssen, Dense single-phase β-Sialon ceramics by glass-encapsulated hot isostatic pressing, J. Mater. Sci. 24 (1998) 1853–1861.
[4] L.K.L. Falk, Z.J. Shen, T. Ekström, Microstructural stability of duplex α-β-sialon ceramics, J. Eur. Ceram. Soc. 17 (1997) 1099–1112.
[5] T. Ekström, Effect of composition, phase content and microstructure on the performance of yttrium sialon ceramics, Mater. Sci. Eng. A109 (1989) 341–349.
[6] C. Zhang, W.Y. Sun, D.S. Yan, Optimizing mechanical properties and thermal stability of Ln-α-β-Sialon by using duplex Ln elements (Dy and Sm), J. Eur. Ceram. Soc. 19 (1999) 33–40.
[7] N. Camuscu, D.P. Thompson, H. Mandal, Effect of starting composition, type of rare earth sintering additive and amount of liquid phase on α⇆β sialon transformation, J. Eur. Ceram. Soc. 17 (1997) 599–613.
[8] H. Mandal, N. Camuscu, D.P. Thompson, Composition of the effectiveness of rare-earth starting additives on the high-temperature stability α-sialon ceramics, J. Mater. Sci. 30 (1995) 5901–5909.
[9] H. Mandal, D.P. Thompson, Reversible α⇆β sialon transformation in heat-treatment sialon ceramics, J. Eur. Ceram. Soc. 12 (1993) 421–429.
[10] Z.J. Shen, T. Ekström, N. Nygren, Homogeneity region and thermal stability of neodymium-doped α-sialon ceramic, J. Am. Ceram. Soc. 78 (1996) 721–732.
[11] G.R. Anstis, P. Chantikul, B.R. Lawn, D.B. Marshall, A critical evaluation of indentation techniques for measuring fracture toughness, J. Am. Ceram. Soc. 64 (1981) 533–538.
[12] T.S. Sheu, Microstructure and mechanical properties of in situ β-Si_3N_4/α′-sialon composite, J. Am. Ceram. Soc. 77 (9) (1994) 2345–2353.
[13] I.W. Chen, A. Rosenflanz, A tough sialon ceramic based on α-Si_3N_4 with a whisker-like microstructure, Nature (London) 389 (1997) 701–704.

[14] J. Kim, A. Rosenflanz, I.-W. Chen, Microstructure control of in-situ-toughened α-sialon ceramics, J. Am. Ceram. Soc. 83 (7) (2000) 1819–1821.
[15] C.A. Wood, H. Zhao, Y.B. Cheng, Microstructure development of calcium α-sialon ceramics with elongated grains, J. Am. Ceram. Soc. 82 (2) (1999) 421–428.
[16] H. Mandal, M.J. Hoffmann, Hardness and toughness of α-sialon ceramics, Mater. Sci. Forum 325–326 (2000) 219–224.